Journal of Catalysis **185,** 1–11 (1999)
Article ID jcat.1999.2478, available online at http://www.idealibrary.com on IDEAL®

Catalytic Activity of Reduced $MoO_3/\alpha\text{-}Al_2O_3$ for Hexanes Reforming

I. Preparation, Characterization, and X-Ray Photoelectron Spectroscopy Studies

F. Barath, M. Turki, V. Keller,[1] and G. Maire

Laboratoire d'Etude de la Réactivité Catalytique, des Surfaces et Interfaces, UMR 7515 du CNRS, Université Louis Pasteur-ECPM,
25, rue Becquerel, BP 08, 67087 Srasbourg Cedex 2, France
E-mail: vkeller@chimie.u-strasbg.fr

Received January 8, 1999; revised March 4, 1999; accepted March 4, 1999

Different $MoO_3/\alpha\text{-}Al_2O_3$ catalyst samples have been prepared using two preparation methods for a MoO_3 deposit, the first one consisting of aqueous impregnation with sodium molybdate and the second one starting from MoO_3 by an equilibrium adsorption in slurry MoO_3/water (called the SIM method: slurry impregnation or solvent assisted spreading method). The α-alumina support was obtained by heating γ-alumina at 1150°C. γ-alumina partially transformed to α-alumina by heating is used as catalyst support. For each kind of preparation two catalyst samples with different MoO_3 loadings were prepared: 0.08 (around 0.04 equivalent monolayer) and 5.4 wt% (around 2.5 equivalent monolayers) and 1.2 (around 0.6 equivalent monolayer) and 5.2 wt% (around 2.4 equivalent monolayer) MoO_3, respectively. They were characterized by X-ray diffraction, temperature programmed reduction, and X-ray photoelectron spectroscopy (XPS) measurements. *In situ* **XPS measurements as a function of reduction time and temperature were performed and compared on the 5.4% $MoO_3/\alpha\text{-}Al_2O_3$ and 1.2% $MoO_3/\alpha\text{-}Al_2O_3$ catalyst samples. The original oxidic form of each catalyst sample, before any reduction treatment, shows only the presence of Mo(VI) surface species. For high molybdenum concentrations, the complete disappearance of Mo(VI) into Mo(V) and Mo(IV) has been observed after treatment for 9 h under hydrogen at 350°C. After reduction for 5 h at 450°C, Mo(0) appeared. For concentrations close to the monolayer, treatments for 10 h under hydrogen at 450°C are necessary to reduce completely Mo(VI) into Mo(V) and Mo(IV); in that case, even a reduction at 700°C is insufficient to observe Mo(0) and only Mo(IV) and Mo(II) surface species are detected. Thus, increasing MoO_3 loading results in an increase of the catalyst reducibility. No $Al_2(MoO_4)_3$ seems to be present before and after reduction steps. Interaction of molybdenum oxide with alumina is discussed, depending on the molybdenum oxidic contents and on the preparation of the catalysts.** © 1999 Academic Press

Key Words: **supported molybdena catalysts; α-kind alumina; reducibility;** *in situ* **XPS measurements; characterizations.**

I. INTRODUCTION

Molybdenum oxides supported on alumina are active in a great number of reactions such as isomerization (1), metathesis, ethylene polymerization (2), and hydrodesulfurization (3, 4). The hydrotreating over the sulfidic molybdenum-based catalyst belongs to the most important application of these catalysts because of their high resistance to sulfur poisoning.

The interaction of molybdenum oxides with alumina and the formation of an oxidized molybdenum monolayer have been the subject of many investigations. Among preparations reported in the literature, impregnation of alumina using ammonium heptamolybdate (5) followed by calcination has been the most widely used (6), although alternative methods have been reported like solid–solid wetting (7, 8) (thermal spreading of MoO_3) or gas phase adsorption of $Mo(CO)_6$. Recently, a new method (9, 10) called SIM (slurry impregnation method) has been reported starting from MoO_3 powder.

The surface chemistry of supported molybdenum oxide catalysts has received much attention (11). In most reactions, catalyst activation requires a reduction step. The resulting activity depends strongly on the extent of reduction of the MoO_x phases, suggesting that the active sites are associated with specific Mo oxidation states. Thus, a correlation between the catalytic activity and different oxidation states has been attempted for benzene hydrogenation (12), for propene hydrogenation and propane hydrogenolysis (13), or for alkene epoxidation (14). Several molybdenum–alumina interaction species and their dependencies on the loading of molybdenum have been proposed (15).

The γ-alumina heated at 1150°C is mainly converted to an α-like-alumina, which is similar to an α-alumina (corundum), but is slightly different in structure. Moreover it is more basic than both α-alumina and γ-alumina and has a surface area slightly greater than the former. It has already been found (16), in the case of tungsten oxides, that this

---

[1] To whom correspondence should be addressed.

0021-9517/99 $30.00
Copyright © 1999 by Academic Press
All rights of reproduction in any form reserved.

high temperature treated γ-alumina when used as support is more efficient for isomerization of linear alkenes into branched chain alkenes than a γ-alumina, resulting probably from some specific interactions of molybdena (leading to the formation of irreductible compounds) with the basic sites of the support. This is the reason in our study isomerization of hexanes and hexenes will be performed using this α-like-alumina as a support (Part II). Comparisons of the reducibility as well as of the catalytic activities for hydrocarbons conversion starting either from α-like-alumina suppport or from a classical γ-alumina support are in course and will be published later. In addition, the use of this α-alumina (corundum) close packed structure will allow us easier modelization studies than starting from a γ-alumina.

This paper will mainly focus on the preparation of MoO_3 supported on α-alumina using two preparation methods, the first one consisting of aqueous impregnation with sodium molybdate (17) and the second one starting from MoO_3 (SIM method) (9, 10). For each kind of preparation, catalyst samples with different MoO_3 loadings have been prepared and characterized. *In situ* XPS (X-ray photoelectron spectroscopy) measurements as a function of reduction time and temperature have been performed, allowing a detailed study of the reducibility of the different catalyst samples.

Correlation with the reactivity of 2-methylpentane and 4-methyl-1-pentene have been carried out and are presented in Part II, as well as a more detailed mechanistic approach using different probe reactants and ^{13}C tracer-labeled hydrocarbons.

II. EXPERIMENTAL METHODS

II.1. Catalyst Preparation

II.1.1. *Preparation of the Catalyst Support*

The α-Al_2O_3 catalyst support was prepared by heating a γ-Al_2O_3 (Woelm Pharma) having initially a surface area of 190 m^2/g according to the following procedure:

—the support was dried at 200°C for 3 h
—it was then heated from 200 to 800°C (10°C/min)
—the temperature was maintained at 800°C for 25 min
—the temperature was raised rapidly from 800 to 1150°C (35°C/min)
—the temperature was kept constant at 1150°C for a short time (10 min).

II.1.2. *Preparation of the Supported Samples*

II.1.2.1. By impregnation with Na_2MoO_4 (17). Sodium molybdate, Na_2MoO_4, was dissolved in water and the solution added to α-Al_2O_3. The mixture was then stirred with magnetic agitation for 18 h at 60°C. After decantation, concentrated nitric acid was added and the solution was warmed 20 min at 80°C. Then the solid was washed with 1 M nitric acid and heated 1 h at 80°C. The solid was then decanted and the operation repeated three times. The catalyst was dried overnight at 110°C and calcinated at 450°C for 3 h.

Two samples were prepared by varying MoO_3 loadings:

—0.08% MoO_3/α-Al_2O_3, denoted Cat1a
—5.4% MoO_3/α-Al_2O_3, denoted Cat1b.

II.1.2.2. By slurry impregnation method (9, 10). MoO_3 was put in water. The slurry of the carrier and MoO_3 was refluxed 6 h at 100°C and shacked every 15 min. The mixture was left standing 15 h at room temperature and the next day it was heated at 95–100°C for 1 h. After decantation the catalyst was dried at 200°C. No calcination was necessary using this method of preparation.

Two catalyst samples were prepared with different MoO_3 contents:

—1.2% MoO_3/α-Al_2O_3, denoted Cat2a
—5.2% MoO_3/α-Al_2O_3, denoted Cat2b.

II.2. Apparatus and Procedures

The XPS measurements were performed in a static system. The reduction and XPS measurements were carried out in a UHV chamber with XPS and AES facilities without putting the sample in air between hydrogen treatments and XPS measurements. An isolation cell housed within the main chamber allows treatments up to atmospheric pressure. The catalyst sample of about 300 mg of powder was pressed in a disk of 8 mm diameter and 1 mm thick under a pressure of 15 kg/cm^2 and placed on a platinum holder heated by direct Joule effect. The temperature was measured by a chromel–alumel thermocouple fixed on the holder. For each reduction step, 760 Torr ($1 \text{ Torr} = 133.3 \text{ N} \cdot \text{m}^{-2}$) of pure hydrogen were introduced into the cell and then the desired reduction temperature was achieved. The reduction temperatures were 350, 450, and 700°C. The surface species were determined by XPS before and after reduction by hydrogen and allowed us to follow the molybdenum oxidation states as a function of time and temperature of reduction.

Commercial $Al_2(MoO_4)_3$ (Strem Chemical) was used as a reference for catalytic tests and for XPS measurements.

III. CHARACTERIZATIONS RESULTS

III.1. BET Determination

The BET measurements have been performed before and after catalytic experiments on an automatic Coulter SA 3100 apparatus and are reported in Table 1 for the four samples. The amounts of catalyst used are between 200 and 500 mg. The surface area of the α-like-alumina used as support was around 18 m^2/g.

TABLE 1

Evolution of BET (m^2/g) Surface Areas before and after Catalytic Tests and Reduction Treatments

	Before catalytic tests	After reduction at 350°C + catalytic tests	After reduction at 450°C + catalytic tests	After reduction at 600°C + catalytic tests
Cat1a	18	20	20	19
Cat1b	15	17	17	12
Cat2a	18	19	20	20
Cat2b	16	18	18	12
$Al_2(MoO_4)_3$	<1	/	30	40

Starting from these specific surface areas and with the supposition that one MoO_3 molecule occupies 20 Å^2 (7), the number of MoO_3 atom/cm^2 as well as the number of equivalent of monolayer can be deduced (Table 2). For low MoO_3 concentrations, specific surface areas are unchanged after treatment by hydrogen and catalytic experiments, independent of the reduction temperature. For higher MoO_3 concentrations (Cat1b and Cat2b with MoO_3 content $>$ equivalent monolayer), surface areas decrease slighly after reduction treatments at 600°C. However, starting from molybdenum aluminate, its surface area increases after treatments by hydrogen.

III.2. X-Ray Diffraction

X-Ray diffraction measurements were made on a Siemens D5000 diffractometer equipped with a goniometer. The incident wave consisted of monochromatic Cu ($\lambda = 1.5418$ Å). The peaks attribution is possible using the Diffract at. software including JCPDS data. X-Ray diffraction patterns of Cat1b, Cat2b, and $Al_2(MoO_4)_3$ before and after catalytic tests and hydrogen reductions were performed:

—The catalyst support is mainly composed of α-Al_2O_3 (corundum) and of traces of κ-alumina

—Catalyst samples Cat1a and Cat2a did not show any molybdenum oxidic phase because of their low MoO_3 loading.

—Concerning Cat1b and Cat2b, which molybdenum oxide loading corresponds to around 2.5 monolayers, a MoO_3 phase was detected.

—However, for the commercial $Al_2(MoO_4)_3$ after 4 h/H_2 at 350°C, 1 h/H_2 at 600°C, and the corresponding catalytic tests at 350°C, XRD patterns reveal the presence of MoO_2 and metallic molybdenum phases. It also seems that aluminum molybdate undergoes a phase separation, followed by a further reduction.

—No bulk aluminium molybdate $Al_2(MoO_4)_3$ was present on the initial catalyst samples and after reduction treatments.

III.3. Temperature Programmed Reduction Data

Temperature programmed reduction (TPR) measurements were carried out on an automatic XSORB (Gira) apparatus. Respectively, 0.5 and 1.0 g of catalyst samples Cat1b and Cat2a were placed in a quartz reactor. The catalyst sample was reduced in a stream of 5% H_2/Ar at a constant flow rate. The reduction temperature was increased from room temperature up to 900°C with a uniform heating of 5°C/min. The H_2 consumption was measured with a thermal conductivity detector. TPR patterns of Cat1b (5.4% MoO_3/α-Al_2O_3) and Cat2a (1.2% MoO_3/α-Al_2O_3) are compared in Fig. 1.

Depending on the molybdenum oxide content, two or three reduction peaks are observed. For a catalyst with a relatively low molybdenum content (Cat2a), two reduction peaks are detected: the first one (the biggest) at 475°C and the second one at 565°C. On Cat1b, these two reduction peaks are also observable but slightly shifted in reduction temperatures: the first reduction peak appears at around 495°C and the second one at around 550°C. Moreover, the relative contributions of the two peaks depend on the

TABLE 2

Geometric Characterization of Catalyst Samples

Catalysts	Cat1a (0.08%)	Cat1b (5.4%)	Cat2a (1.2%)	Cat2b (5.2%)
Surface area (m^2/g)	18	15	18	16
Mo/cm^2	1.7×10^{13}	1.3×10^{15}	2.8×10^{14}	1.2×10^{15}
Equivalent monolayer	0.04	2.50	0.60	2.40
Surface species	Monomeric Td difficult to reduce (15)	Bulklike (15, 22) easy to reduce	Monomeric Td + Polymolybd. Oh (22)	Bulklike (15, 22) easy to reduce

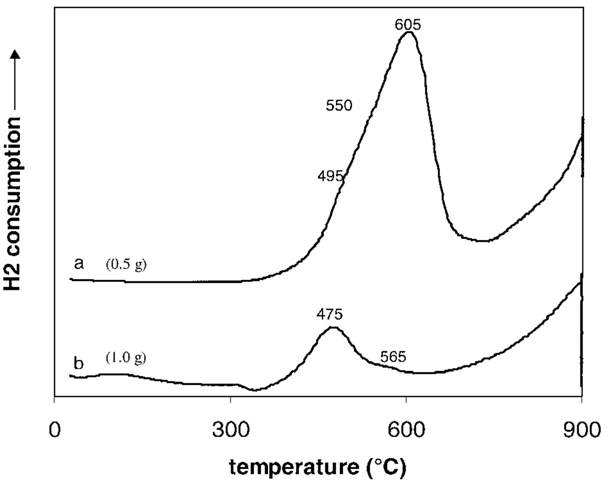

FIG. 1. TPR profiles of (a) Cat1b (130×10^{13} Mo/cm^2) and (b) Cat2a (28×10^{13} Mo/cm^2).

molybdenum concentration of the catalysts, the most important peak for Cat2a being the first, whereas it is opposite for Cat1b. It can be observed that the reduction temperature of the first peak increases and that of the second peak decreases, respectively, with the increase of the molybdenum content from 28 to 130 Mo/cm^2.

A third reduction peak, whose area is the most important, emerges at 605°C for the sample with the highest molybdenum content (Cat1b). It must be noted that, proportional to the catalyst weight used for TPR, the surfaces of the peaks are much more important for Cat1b than for Cat2a, meaning that for the former the extent of reduction increases with increasing the molybdenum content. Similar TPR spectra have already been reported in the literature (15) on MoO_3/Al_2O_3 showing a simple reduction peak at around 460°C for catalysts containing less than 25×10^{13} Mo/ cm^2 and the appearance of a double peak of reduction at a molybdenum concentration around 30×10^{13} Mo/ cm^2, growing quickly with the increase of molybdenum content. Furthermore the third peak at 605°C has already been observed as a shoulder clearly distinguished on 12% molybdena/γ-alumina samples (18).

The first reduction peak at 475–495°C can certainly be attributed to the reduction of Mo(VI) in octahedral coordination to Mo(V). The second TPR peak at 550–565°C can be assigned to the reduction in Mo(IV). It has already been noted (11) that the Al_2O_3 support contributes to a better reduction of Mo(VI) to Mo(V) and to the stability of Mo(V). That seems to be the reason why the corresponding peak appears at a lower temperature for Cat2a than for Cat1b and why its relative contribution compared to the second reduction peak is more important for the former. Moreover, that is why the area of the second peak assigned to the reduction in Mo(IV) is greater and why it appears earlier for Cat1b, whose geometric characterization is close to a bulk-like catalyst.

The third reduction peak at 605°C, only detected on the catalyst sample with the highest molybdenum content (Cat1b), can be attributed to a further reduction in metallic molybdenum not observed on Cat2a.

Another reduction peak at temperatures greater than 900°C can correspond to some reduction of the carrier certainly assisted by hydrogen dissociation on molybdenum species showing metallic properties, such as Mo(IV) or Mo(0). The intensity of this peak seems to become stronger by increasing the molybdenum content.

III.4. X-Ray Photoelectron Spectroscopy (XPS)

Selection for binding energies' references. All the catalysts studied are insulators, and thus produce charging effects. It was necessary to fix a reference for the binding energies' determinations. The most often cited reference is the carbon due to contamination at 284 eV (1s level). However, the carbon peak can be poorly defined and it can exist in different chemical forms. Thus, the shift of the C1s peak due to charging effects may be different from the displacement of the other peaks, which can give rise to incoherent results. So, we chose the Al 2s level of the α-Al_2O_3 (19) carrier as a reference (119.6 eV).

III.4.1. Cat1b: 5.4% MoO_3/α-Al_2O_3

As the catalyst precursor of Cat1b was sodium molybdate, XPS spectra of the Na1s region are given in Fig. 2 as a function of reduction time and temperature. It has been shown that the calcined sample exhibits no detectable sodium traces at the surface. Nevertheless, the sodium amount rises at the surface as the time and reduction temperature increase.

The XPS of the Mo3d energy region of calcined Cat1b (Fig. 3) shows the presence of only one state of molybdenum: the Mo(VI) identified at 232.6 and 235.8 eV for the Mo3d spin–orbit component. After 9 h/H_2 at 350°C (b), the

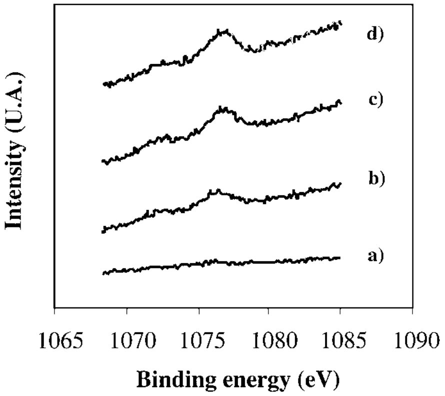

FIG. 2. XPS spectra of the Na1s region of Cat1b. (a) Calcined sample, (b) after 2 h/H_2 at 350°C, (c) after (b) + 23 h/H_2 at 350°C, (d) after (c) + 3 h/H_2 at 450°C.

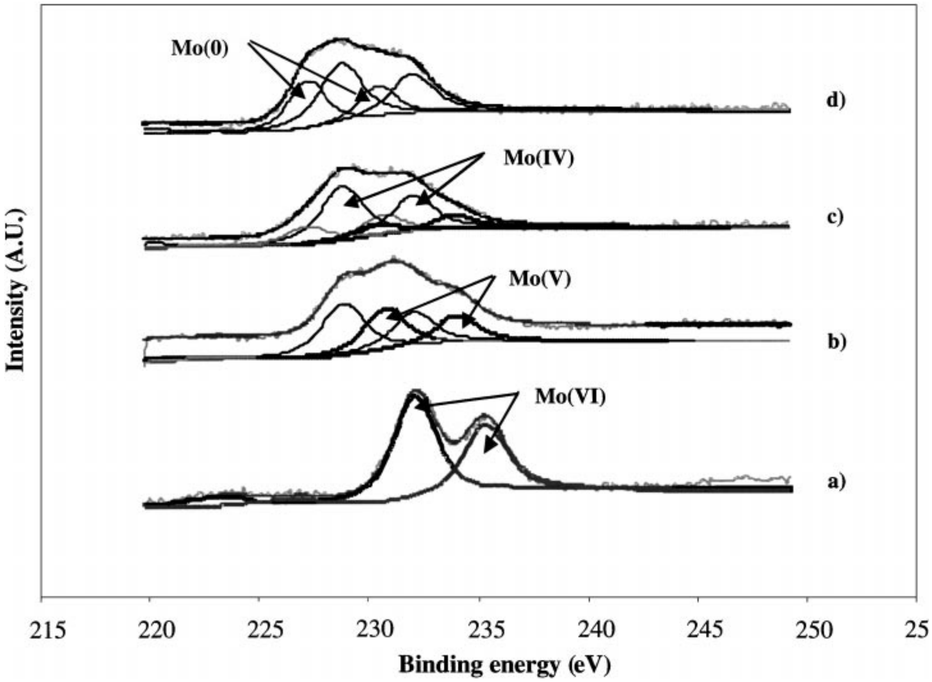

FIG. 3. XPS spectra of the Mo3d region of Cat1b. (a) Calcined sample, (b) after 9 h/H_2 at 350°C, (c) after (b) + 16 h/H_2 at 350°C + 5 h/H_2 at 450°C, (d) after (c) + 1 h/H_2 at 700°C.

spectrum shows a more complex structure. Curve fitting reveals the disappearance of all the Mo(VI) oxidation state and the appearance of Mo(V) and Mo(IV) spin–orbit components, respectively, at 231.5 and 234.7 eV and at 229.7 and 232.9 eV. Further reduction (c) shows, in addition to Mo(V) and Mo(IV), the presence of Mo(0) states at 227.9 and 231.1 eV. Continuing reduction at 700°C (d) almost total disappearance of MoV (5.0%); the only molybdenum species remaining are Mo(IV) (60.0%) and Mo metallic (35.0%). It must be noted that the charging effect is about 3.8 eV for the initial catalyst and that it varies between 4.0 and 5.5 eV as a function of different reduction treatments.

Kinetics of reduction at 350 and 450°C. The evolution of surface Mo species as a function of reduction time at 350 and 450°C is shown in Figs. 4a and 4b, respectively. It can be shown that Mo(VI) is not any more detectable after 9 h/H_2 at 350°C. Concerning Mo(V), its concentration increases rapidly to a maximum and then decreases all the more rapidly once the reduction temperature is increased. After 4 h/H_2 at 350°C the decay of Mo(V) is accompanied

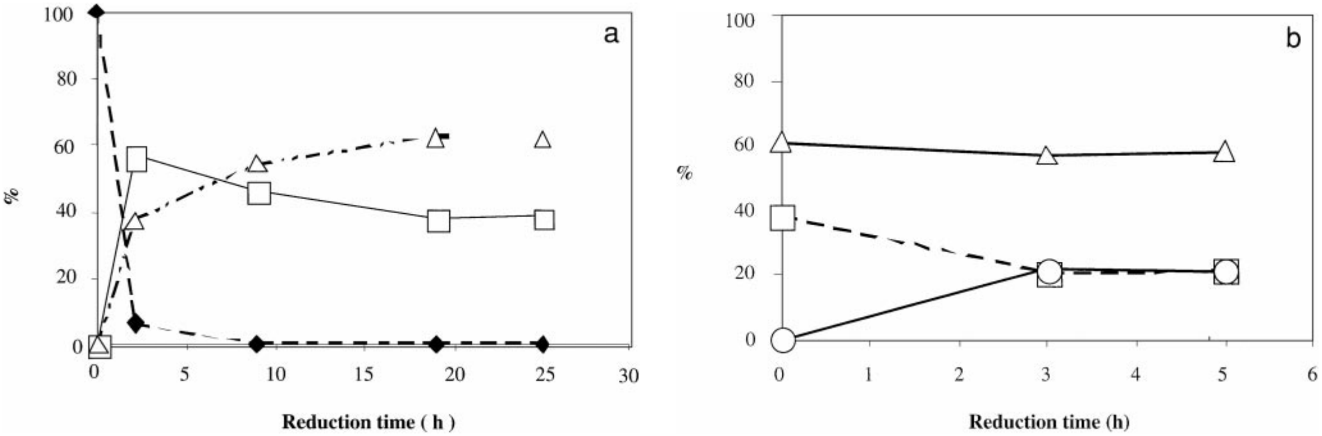

FIG. 4. Distribution of Mo surface species: Mo(VI) (◆), Mo(V) (□), Mo(IV) (△) and Mo(0) (O) versus reduction time (h) (a) at 350°C and (b) at 450°C.

TABLE 3

$C_{\mathrm{Mo}}/C_{\mathrm{Al}}$ Surface Ratios as a Function of Reduction Treatments/H_2 on Cat1b

Treatment	$C_{\mathrm{Mo}}/C_{\mathrm{Al}}$
Initial	0.24
2 h/H_2 at 350°C	0.23
9 h/H_2 at 350°C	0.26
25 h/H_2 at 350°C	0.24
previous + 3 h/H_2 at 450°C	0.22
previous + 2 h/H_2 at 450°C + 1 h/H_2 at 700°C	0.21
previous + 1 h/H_2 at 700°C	0.23

by an inverse increase of Mo(IV), which is kept constant even after 5 h/H_2 at 450°C. Metallic molybdenum rapidly appears after a few hours reduction at 450°C.

Surface concentration ratios. The surface concentration ratios $C_{\mathrm{Mo}}/C_{\mathrm{Al}}$ are given in Table 3 for the initial catalyst and after each reduction treatment. An examination of the surface concentration ratios shows that hydrogen treatments at increasing times and temperatures do not change the surface by agglomeration (coalescence) in larger particles or by redispersion of the molybdenum oxidic phases.

III.4.2 Cat2a: 1.2% $MoO_3/\alpha\text{-}Al_2O_3$

As for the previous sample, the XPS spectra of Cat2a dried at 200°C reveals only one kind of molybdenum species (Fig. 5a) at 232.6 and 235.8 eV, characteristic of the two spin–orbit components of Mo(VI) oxidation state. But, in contrary to the previous sample (Cat1b), a reduction at 350°C (Fig. 5b) for 9 h does not allow the complete reduction of Mo(VI) since 27% are still detectable after this treatment. However, Fig. 5b reveals the appearance of Mo(V) and Mo(IV) surface species. The complete reduction of Mo(VI) needs a higher temperature reduction, i.e., 10 h at 450°C (c); this reduction at 450°C results only in the presence of Mo(V) and Mo(IV), but no metallic Mo has been detected (as it was for Cat1b). Further reduction at 700°C shows the appearance of the two spin–orbit components of Mo(II) surface species at 228.5 and 231.7 eV (13). Even after 1 h/H_2 at 700°C no metallic Mo surface species have been detected, although for Cat1b, 35.0% of Mo(0) has been measured. In this case the charging effect goes from 4 to 5.5 eV for different reduction treatments.

It can be concluded, comparing Cat1b and Cat2a, that the second one, which contains the lowest molybdenum loading, is, as expected, more difficult to reduce. Recent XPS studies of molybdena–alumina catalysts (12% $MoO_3/\gamma\text{-}Al_2O_3$) (20) have shown that reduction at 400°C only gives Mo(V) and Mo(IV) species, confirming that the reducibility strongly depends on the presence of a rather bulklike structure or of a surface layer. Even at 700°C, no metallic molybdenum state is observed.

Kinetics of reduction. At 350°C (Fig. 6a), the Mo(VI) surface concentration decreases rapidly during the first 2 h

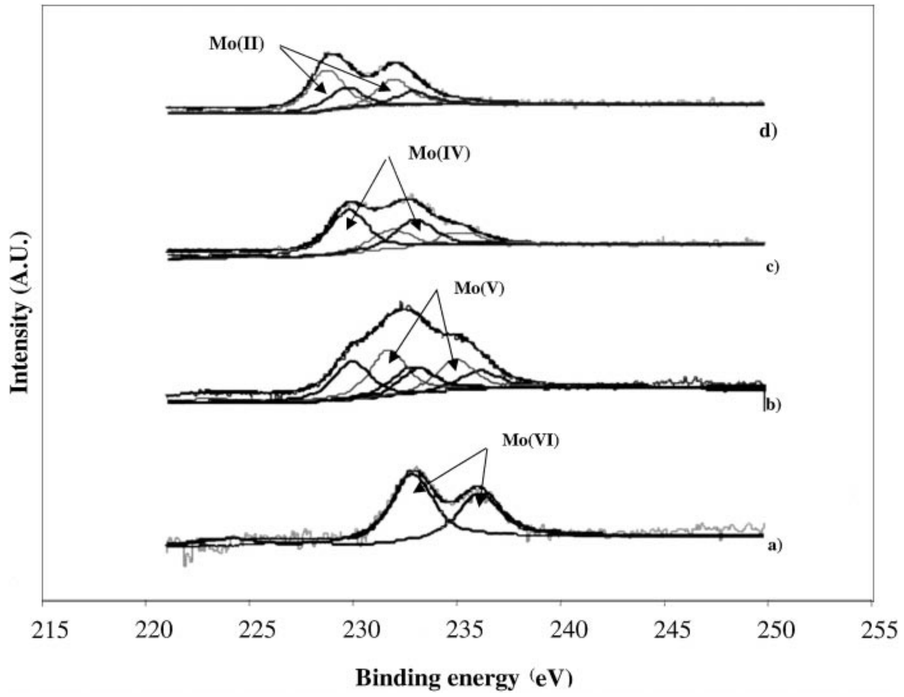

FIG. 5. XPS spectra of the Mo3d region of Cat2a. (a) Dried at 200°C, (b) After 9 h/H_2 at 350°C, (c) After (b) + 16 h/H_2 at 350°C + 10 h/H_2 at 450°C, (d) After (c) + 1 h/H_2 at 700°C.

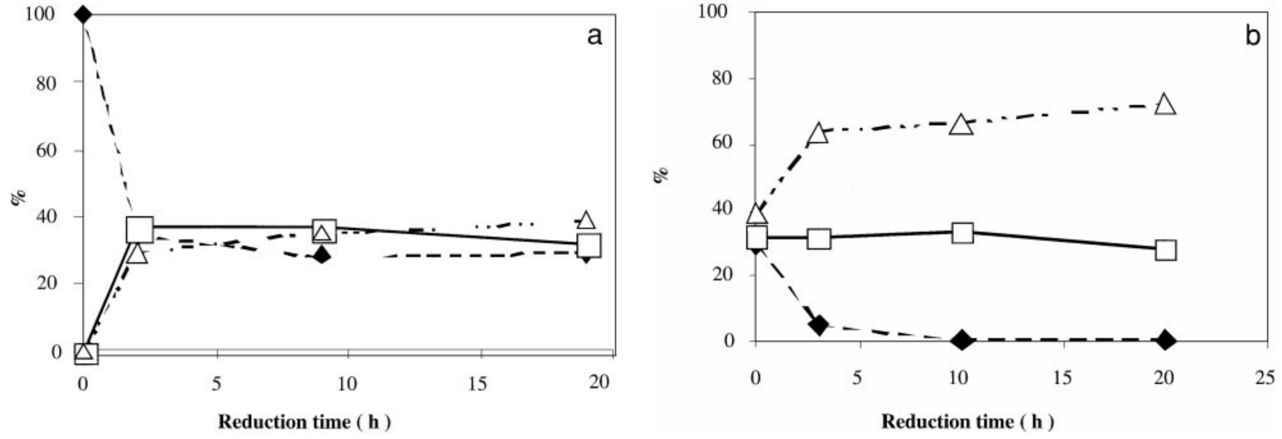

FIG. 6. Distribution of Mo surface species: Mo(VI) (◆), Mo(V) (□), Mo(IV) (△) versus reduction time (h) (a) at 350°C and (b) at 450°C.

of reduction, accompanied at the same time by an increase of Mo(V) and Mo(IV). Then the Mo(VI) contribution continues to decrease slightly with the reduction time at 350°C. Mo(V) and Mo(IV) display reverse monotonic variations with time on reduction at 350°C.

At higher temperature (Fig. 6b), appreciable Mo(IV) is formed earlier in the reduction, whereas only a slight decrease of Mo(V) is observed. The appearance of Mo(IV) seems to be correlated with the disappearance of Mo(VI). At 450°C no metallic molybdenum has been detected.

To get more informations about the reducibility of Mo(VI), which is the only state present on the dried catalyst before reduction, and about its behavior during thermal heating, Cat2a was heated under helium. Figure 7 clearly shows that a treatment by an inert gas (2 h under Helium at atmospheric pressure) at 350°C results in the partial transformation of Mo(VI) into Mo(V) to yield around 30% of Mo(V) species. Continuing this treatment 1 h under helium at atmospheric pressure at 600°C does not affect the surface states of molybdenum any more.

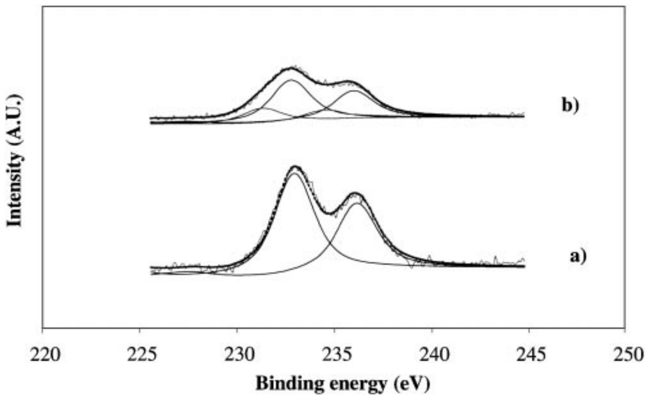

FIG. 7. XPS spectra of the Mo3d region of Cat1b. (a) Dried at 200°C and (b) after 2 h/Helium at 350°C.

Thus, a thermal heating seems to be enough to convert partly Mo(VI) into Mo(V) species.

Surface concentration ratios. Comparing to Cat1b (5.4% MoO_3/Al_2O_3 (Table 3)), the surface concentration ratios, C_{Mo}/C_{Al}, are two times lower for Cat2a (1.2% MoO_3/Al_2O_3 (Table 4)), but as previously, different hydrogen treatments do not affect these ratios and thus do not yield to a modification of the surface morphology.

III.4.3. Commercial $Al_2(MoO_4)_3$

As it appears from the X-ray diffraction pattern that aluminum molybdate treated 4 h/H_2 at 350°C and 1 h/H_2 at 600°C leads to phase separation to give molybdenum oxidic phases and metallic molybdenum, a more detailed XPS study was performed. It consists of heating this sample in an inert gas, helium, to follow the evolution of the molybdenum surface species and to see if only a thermal heating is enough to yield the phase separation. The different molybdenum species binding energies, composition, and the charging effect, as well as the surface ratios C_{Mo}/C_{Al} as a function of temperature treatment by helium are reported in Table 5.

TABLE 4

C_{Mo}/C_{Al} Surface Ratios as a Function of Reduction Treatments/H_2 on Cat2a

Treatment	C_{Mo}/C_{Al}
Initial	0.10
2 h/H_2 at 350°C	0.13
9 h/H_2 at 350°C	0.09
19 h/H_2 at 350°C	0.10
previous + 10 h/H_2 at 450°C	0.11
previous + 10 h/H_2 at 450°C + 2 h/H_2 at 600°C	0.12
previous + 5 h/H_2 at 600°C	0.11
previous + 1 h/H_2 at 700°C	0.10

TABLE 5

Binding Energies (BE) (eV), Charging Effects, and C_{Mo}/C_{Al} Surface Ratios of $Al_2(MoO_4)_3$ as a Function of Thermal Heating under Helium

Treatment	Mo(VI) BE $3d_{5/2}$ (eV)	Mo(VI) Contribution %	Mo(V) BE $3d_{5/2}$ (eV)	Mo(V) Contribution %	Charging effect (eV)	C_{Mo}/C_{Al}
Initial $Al_2(MoO_4)_3$	232.8	100			2.5	2.8
After 6 h/He at 350°C	232.8	85.8	231.5	14.2	2.8	3.4
After 6 h/He at 350°C + 2 h/He at 600°C	232.8	57.2	231.5	42.8	4.7	5.6

Although the Mo(VI) in $Al_2(MoO_4)_3$ and in the molybdenum catalyst samples studied previously cannot be distinguished by XPS it is not possible to discriminate if after heating under helium molybdenum is present in the chemical surrounding of $Al_2(MoO_4)_3$ or MoO_3. Only the increase of the charging effect as well as the increase of the Mo/Al surface ratios seems to lead to the conclusion that there is a phase separation of $Al_2(MoO_4)_3$ into MoO_3 and Al_2O_3 after a thermal heating by helium. This observation has already been mentioned in the case of $Al_2(WO_4)_3$ (21).

IV. DISCUSSION

Many papers have dealt with the process of deposit of molybdenum oxides on an oxidic carrier like alumina (mainly γ-alumina) and mentioned already the very important influences of interactions between the molybdenum oxidic species and the surface of alumina, depending on the preparation or calcination procedures adopted. Some of these interactions concern:

—the diffusion of Mo cations into the support during the deposition or the calcination step leading to a well-defined compound, like $Al_2(MoO_4)_3$ (22),

—the chemical adsorption of the molybdenum at the alumina surface through the formation of Mo–O–Al bonds yielding to superficial molybdates species (23–26),

—the presence of the Anderson-type heteropolymolybdate $[Al(OH)_6Mo_6O_{18}]^{3-}$ recently observed. When ammonium heptamolybdate was deposited on γ-Al_2O_3 by the equilibrium adsorption method, this compound is formed in the solution and issued from reactions between molybdates ions and aluminium species coming from the support dissolution and also present on the solid catalyst after deposition (27). However, studies concerning the thermal transformations of this Anderson-type heteropolymolybdate during calcination or reduction have not been published yet.

—the growth of three-dimensional MoO_3 aggregates onto the surface of Al_2O_3.

Formation of the $Al_2(MoO_4)_3$ Defined Compound

Although some authors have already observed using ^{95}Mo NMR (28) and MAS ^{27}Al NMR (29) that at high molybdenum loading stable $Al_2(MoO_4)_3$ is present as a minor species and that a “subsurface” $Al_2(MoO_4)_3$ phase is present in some cases after calcination some other authors contested the presence of bulk $Al_2(MoO_4)_3$ (26, 30). On the other hand, Imamura (31) has observed that when calcination temperature was increased from 500 to 650°C, $Al_2(MoO_4)_3$ was produced only on γ- and χ-aluminas, while it was not formed on α-alumina. Moreover, on tungsten oxide-supported catalysts (16), it has been noted that even if the formation of bulk $Al_2(WO_4)_3$ is expected at calcination temperatures above 1100°C, it is unlikely that such a compound could be formed at lower temperature, like calcination temperatures of 450°C used in some cases in this work.

In our case the XRD experiments have shown that bulk aluminum molybdate is not present on the initial catalysts. It has been shown that, even if it were present but undetectable by X-ray (small discrete crystallites or in an amorphous form) it should be reduced faster than the bulk $Al_2(MoO_4)_3$ (26). Even if after calcination such a compound would have been formed, it has been shown in this paper that a thermal heating is enough to decompose it into MoO_3 and Al_2O_3; a further reductive treatment easily leads to MoO_2 and metallic Mo, observed by X-ray diffraction. Such a phase separation has already been demonstrated starting from $Al_2(WO_4)_3$ (21).

Formation of Superficial Molybdate Species

The majority of supported Mo catalysts is prepared by deposition of ammonium heptamolybdate, which is transformed into molybdates ions interacting with the alumina surface. Different ways of adsorption of molybdates species have been proposed in the literature such as:

—an electrostatic model (32) considering the charge of the ion, the pH of the impregnation solution, and the isoelectric point (IEP). But it has been shown (33) that a simple electrostatic model cannot only account for adsorption of these anions especially when the pH of the solution is higher than the IEP.

—the exchange (or reaction) of the surface hydroxyl groups of alumina by molybdates ions, these hydroxyl groups being protonated or not, depending on the value of the pH. It must be noted that the predominant molybdates ions present in solution at various pH can be represented as

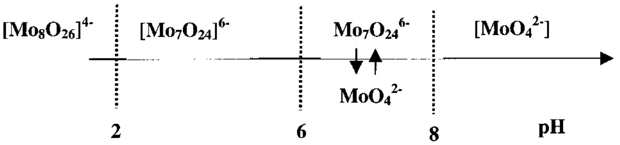

[1]

For 6<pH<8, the following well-known equilibrium between hepta- and monomolybdates anions must be considered:

$$MoO_7O_{24}^{6-} + 4H_2O \Leftrightarrow 7MoO_4^{-} + 8H^{+} \qquad [2]$$

It has been shown that at very low molybdenum loading (30, 34, 35) (<10^{13} Mo/cm^2) MoO_4^- is preferentially adsorbed (exchanged) on the basic hydroxyl groups present on alumina and thus tetrahedral monomeric molybdates species are present on the surface, this species being reduced with difficulty. Molybdenum species in octahedral coordination are formed at >9 × 10^{13} Mo/cm^2 with a progressive increase in the proportion as molybdenum content increases (15); these octahedral molybdate species constitute polymolybdates with various degrees of aggregation. The way of formation of these octahedral polymolybdates species is very controversed in the literature. It is well established that molybdenum species are well dispersed up to a molybdenum surface concentration of (40–60) × 10^{13} Mo/cm^2 (below 0.75 monolayer) (15).

Growth of Three-Dimensional MoO_3 Aggregates onto the Surface of Al_2O_3

A further increase of the molybdenum loading (>monolayer) resulting in a decrease of the interactions between molybdenum species and the alumina support leads to the formation of three-dimensional aggregates of MoO_3, whose reduction is different.

Thus, the reducibility of the surface of the different catalyst samples depends strongly on the preparation methods and conditions used, on the molybdenum loading, on the different kind of surface species present, on their interaction with the support, and on the presence or absence of calcination, as well as on the calcination temperature.

Influence of the Preparation Method

In our case, two preparation methods have been used, the first one consisting of impregnation of the alumina support with a Na_2MoO_4 and the second one using a slurry impregnation method starting from bulk MoO_3 in solution.

—for the first preparation method, the initial sodium tungstate solution was slightly basic (>8), so that the predominant species were MoO_4^{2-} according to Eq. [1]. After addition of concentrated nitric acid, molybdic acid was formed and the pH decreases to values<2. As it has already been proposed by Dufaux and Che (36), it can be supposed that during the impregnation, the most basic OH groups from the alumina surface would react with the molybdic acid, H_2MoO_4, leading to tetrahedral monomeric molybdates species, following the scheme

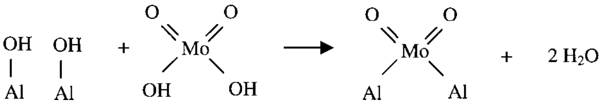

[3]

Thus, it can be supposed using this preparation method, that initially tetrahedral monomeric molybdate species which are reduced with difficulty are formed even more easily at the surface, compared to the method of preparation with deposition of ammonium heptamolybdate. Two reasons can be invoked: first, the probability of the presence of heptamolybdates species is negligible at the initial pH (basic >8) of the sodium tungstate solution; on the other hand, it has already been noted (36) that molybdic acid reacts only with the most basic hydroxyl groups of the support, the less basic being unaffected. Some polymeric species may perhaps be formed after the calcination treatment. Nevertheless, it is known that at very low pH (<2) octamolybdate species can be formed, which tends to polymerize and eventually to form a precipitate (37).

Concerning residual sodium impurities rising to the surface with reduction treatments, it appears studying WO_x/Al_2O_3 catalysts that these impurities provide the basic sites necessary for $Al_2(WO_4)_3$ or other tungsten complexes to be formed.

—the SIM method consists of the dissolution and equilibrium adsorption of bulk MoO_3 in water. This solubility is low at room temperature (0.1 g/100 ml) but is enhanced with an increase of the temperature (2.1 g/100 ml) at 70°C. In our impregnation conditions (5<pH<7), the initial dissolution of MoO_3 mainly leads to monomeric tetrahedral molybdates species MoO_4^{2-} (38), whose stability is ruled out by Eq. [2]. It has already been demonstrated by Zdražil *et al.* (39) using the SIM method for the preparation of MoO_3/Al_2O_3 catalysts that the stoichiometry of reaction (OH/Mo) is 2 for the range of the lowest Mo loading (<10^{14} at Mo/cm^2), meaning that mainly monomeric tetrahedral molybdates are present. By increasing the Mo loading, a decrease of the OH/Mo stoichiometry is observed, issued from the diminution of the concentration of free OH groups and meaning that formation of dimeric or polymeric structures occurs.

So in order to summarize the different molybdate species present on the surface of our four catalyst samples, depending on the preparation method employed and according to the literature, Table 2 (Sect. III.1.) can be completed.

Reducibility of Our Catalyst Samples

The behaviors of the low Mo loading catalysts, Cat2a (1.2% MoO_3/Al_2O_3) and Cat1a (0.08% MoO_3/Al_2O_3), and of the high loading samples, Cat1b (5.4% MoO_3/Al_2O_3) and Cat2b (5.2% MoO_3/Al_2O_3) during hydrogen treatments are very different:

—it has been shown that the extent of reduction increases with the increase of molybdenum content, as it has been observed using XPS and TPR characterizations. Thus, on Cat1b, Mo(VI) species rapidly disappeared after only a few hours of reduction at 350°C and a reduction at 450°C leads to metallic molybdenum. Concerning Cat2a, even at 700°C no metallic molybdenum has been detected, but mainly Mo(IV) and Mo(II) species.

It can also be deduced from these observations that Cat1b behaves as a bulk-like MoO_3 catalyst. This is confirmed by the TPR profile close to that of bulk MoO_3 because of the predominance of the following reduction steps: MoO_3 (VI) $\rightarrow$ MoO_2 (IV) $\rightarrow$ Mo(0), the formation of intermediate species, like Mo(V), being unfavored. Moreover it has been observed by X-ray diffraction on Cat1b (5.4% MoO_3/Al_2O_3) and Cat2b (5.2% MoO_3/Al_2O_3) that a bulk MoO_3 phase has been detected. Looking at the evolution of BET areas, only the surface areas of the high loaded samples (Cat1b and Cat2b) decreases after reduction at 600°C followed by catalytic test; this observation can be related to the appearance of metallic molybdenum.

On the other hand, it can be interpreted from the results concerning Cat2a that it behaves like a monolayer of molybdates species interacting with the surface. First on Cat2a (1.2% MoO_3/Al_2O_3), as well as on Cat1a (0.08% MoO_3/Al_2O_3), no discrete MoO_x phases have been detected by X-ray diffraction. From XPS measurements and TPR profiles, it can be shown that the reduction of Cat2a does not follow the predominant steps of bulk molybdenum mentioned above, but some intermediate valence states have been detected, like Mo(V) and Mo(II) species. It has already been observed in the literature (26) that alumina appears to have the special property of stabilizing intermediate Mo valence states, in particular, Mo(V). Masson and Nechtschein (40) have postulated that the Mo(V) state is stabilized through a valence induction effect due to the alumina and as such is confined to that layer of Mo immediately adjacent to the alumina surface. So, additional layers of Mo act as free MoO_3 and reduce directly to MoO_2. Furthermore, the heterogeneity of alumina surfaces is well known. Thus, at the beginning of deposition, for the lowest Mo loadings, more active sites (basic) on the alumina may react preferentially with the molybdena, either by adsorption of molybdates ions from solution during impregnation or during calcination, forming stronger interactions than when the adsorption takes place on the less basic OH sites. That is why it can be supposed that Cat1a (0.08% MoO_3/Al_2O_3) should be reduced with more difficulty than Cat2a (1.2% MoO_3/Al_2O_3).

Influence of the Nature of the Alumina Support

It should be evident that the superficial and structural properties of alumina may play an important role on the different interactions existing between molybdenum species and the alumina support and thus on the reducibility of the catalyst samples. Thus, one can believe that the number and density of available surface OH groups, as well as their relative basicity (since acido-basic reactions take place), must play a crucial role on the formation of superficial molybdenum species. Some authors (41) assumed that strongly bonded molybdate and tungstate species may adsorb at the sites occupied by the most basic hydroxyl groups of the alumina. Since alumina has five types of hydroxyl groups (42), the less basic types could be responsible for the adsorption of weakly bounded molybdate and tungstate species. Thus, the heterogeneity of the alumina surface may lead to surface interactions having a variable range of bond strengths. Some other authors (30), comparing the molybdena catalyst supported on γ- and η-Al_2O_3, have supposed that the bridge formation occurring during polymerization must be determined by the structure of the crystallographic planes which are exposed on the alumina surface. Dufaux and Che (36) have observed that the production of Mo(V) is favored on η-Al_2O_3 in comparison to γ-Al_2O_3. It has been mentioned too (43) that the formation of Mo(V) is easier on γ-Al_2O_3 than on α-Al_2O_3. More recently, Imamura *et al.* (31) have noted that when calcination temperature of Mo-loaded aluminas was increased from 500 to 650°C, $Al_2(MoO_4)_3$ was produced on γ- and χ-Al_2O_3, while it was not formed on α-Al_2O_3. Baker *et al.* (16) justified the use of a high temperature treated γ-Al_2O_3 mainly converted to an α-Al_2O_3 corundum structure by the fact that this resultant alumina is more basic than the starting one and than a pure α-corundum one.

It is certain that the kind of alumina used for MoO_x/Al_2O_3 catalyst samples must have a great importance on the interaction of superficial molybdates species with the alumina support, yielding perhaps to differences in reducibility of some molybdenum species, but no consequent modifications have been reported in the overall activity of the catalyst. However, some comparisons between the reducibility and the catalytic activities of MoO_3 supported on pure α-, on γ-, on high heated γ-, as well as of a mixture of α-and θ-Al_2O_3 for alkenes and alkanes reactions are in course.

CONCLUSION

From the different results presented in this paper and in accordance with the literature different conclusions can be pointed out:

1. Whatever the preparation method used or the molybdenum content, it seems that no $Al_2(MoO_4)_3$ phase has been formed not in the initial oxidic form nor after different reduction treatments.

2. The extent of reduction depends mainly on the molybdenum content.

—for high molybdenum loadings (>monolayer) the catalyst samples behave like bulk MoO_3 for reduction.

—for very low molybdenum content, it is very difficult for the catalyst to be reduced because the larger part of adsorbed molybdates species are tetrahedral monomeric ones, which are adsorbed on the most basic hydroxyl groups on the alumina surface.

—for intermediate molybdenum contents (close to monolayer), there is a presence of both tetrahedral monomeric and octahedral polymeric molybdates species. The overall reducibility should also depend on their relative proportion and on the degree of aggregation.

3. The influence of different catalyst precursors, as well as impregnation conditions (pH), or the effect of calcination have been tested too. Nevertheless, the influence of sodium impurities has not been observed. It seems that the SIM method has some advantages like the absence of the calcination step, the adsorption of all the molybdenum species instead of their precipitation into the pores, and the fact that no residual compounds, like sodium or nitrogeneous waste gases, are present when starting, respectively, from Na_2MoO_4 or ammonium heptamolybdate precursors.

REFERENCES

1. Holl, Y., Garin, F., Maire, G., Muller, A., Engelhard, P. A., and Grosmangin, J., *J. Catal.* **104**, 225 (1987).
2. Boreskov, G. K., Dzisko, V. A., Emel-Yanova, V. M., and Pecherskoy, Y. I., *Dolk. Akad. Nank.* **150**, 829 (1963).
3. Luck, F., *Bull. Soc. Chim. Belg.* **100**, 781 (1991).
4. Breysse, M., Portefaix, J. L., and Vrinat, M., *Catal. Today* **10**, 489 (1991).
5. Spanos, N., Vordonis, L., Kordulis, Ch., and Lycourghiotis, *J. Catal.* **124**, 301 (1990).
6. Knözinger, H., “Proceedings, 9th International Congress on Catalysis, Calgary, 1988” (M. J. Phillips and M. Ternan, Eds.), p. 20, Chem. Institute of Canada, Ottawa, 1988.
7. Xie, Y., and Tang, Y., *Adv. Catal.* **37**, 1 (1990).
8. Reddy, B. M., Reddy, E. P., and Srinivas, S. T., *J. Catal.* **136**, 50 (1992).
9. Zdražil, M., *Catal. Lett.* **27**, 337 (1994).
10. Hillerova, E., Morishige, H., Inamura, K., and Zdražil, M., *Appl. Catal. A* **156**, 1 (1997).
11. Massoth, P. E., *Adv. Catal.* **27**, 265 (1978).
12. Yamada, M., Yasamura, J., Houalla, M., and Hercules, D. M., *J. Phys. Chem.* **95**, 7037 (1991).
13. Yasumaru, J., Yamada, M., Houalla, M., and Hercules, D. M., “Proceedings, 10th International Congress on Catalysis, Budapest, 1992” (L. Guczi, F. Solymosi, and P. Tetenyai, Eds.), p. 1867. Akadémiai Kiadó, Budapest, 1993.
14. Morazzoni, F., Canevali, C., D’Aprile, F., Bianchi, C., Tempesti, E., Giuffre, L., and Airodi, G., *J. Chem. Soc. Faraday. Trans.* **91**, 3969 (1995).
15. Okamoto, Y., and Imanaka, T., *J. Phys. Chem.* **92**, 7102 (1988).
16. Chappel, P. J. C., Kibel, M. H., and Baker, B. G., *J. Catal.* **110**, 139 (1988).
17. Baker, B., Clark, J. N., MacArthur, H., and Summerville, E., WO 84/00702 (1984).
18. Dobrovolsky, M., Matusek, K., Paal, Z., and Tétényi, P., *J. Chem. Soc. Faraday Trans.* **89**, 3137 (1993).
19. Oliveros, I., Perez Zurita, M. J., Houalla, M., and Hercules, D. M., *J. Catal.* **171**, 485 (1997).
20. Paal, Z., Tétényi, P., Muhler, M., Wild, U., Manoli, J. M., and Potvin, *J. Chem. Soc. Faraday Trans.* **94**, 459 (1998).
21. Katrib, A., Hemming, F., Hilaire, L., Wehrer, P., and Maire, G., *J. Electron Spectrosc. Relat. Phenom.* **68**, 589 (1994).
22. Zingg, D. S., Makovsky, L. E., Tisher, R. E., Brown, F. R., and Hercules, D. M., *J. Phys. Chem.* **84**, 2998 (1980).
23. Wachs, I. E., *Catal. Today* **27**, 437 (1996).
24. Giordano, N., Castellan, A., and Compadell, F., *J. Catal.* **37**, 204 (1975).
25. Medema, J., Van Stam, C., and Koninsberger, D. C., *J. Catal.* **53**, 386 (1978).
26. Massoth, F. E., *J. Catal.* **30**, 204 (1973).
27. Carrier, X., Lambert, J. F., and Che, M., *J. Am. Chem. Soc.* **119**, 10137 (1997).
28. Edwards, J. C., Adams, R. D., and Ellis, P. D., *J. Am. Chem. Soc.* **112**, 8349 (1990).
29. Mc Millan, M., Brinen, J. S., and Haller, G. L., *J. Catal.* **97**, 243 (1986).
30. Jeziorowski, H., and Knözinger, H., *J. Phys. Chem.* **83**, 1166 (1979).
31. Imamura, S., Sasaki, H., Shono, M., and Kanai, H., *J. Catal.* **117**, 72 (1998).
32. Brunelle, J. P., *Pure Appl. Chem.* **50**, 1211 (1978).
33. Mulcahy, F. M., Fay, M. J., Proctor, A., Houalla, M., and Hercules, D., *J. Catal.* **124**, 231 (1990).
34. Dufresne, P., Payen, E., Grimblot, J., and Bonnelle, J. P., *J. Phys. Chem.* **85**, 2344 (1984).
35. Diaz, A. L., and Bussel, M. E., *J. Phys. Chem.* **97**, 470 (1993).
36. Dufaux, M., Che, M., and Naccache, C., *C. R. Acad. Sci. Paris Ser. C* **268**, 2255 (1969).
37. Van Veen, J. A. R., De Witt, H., Emeis, C. A., and Hendricks, P. A. J. M., *J. Catal.* **107**, 579 (1987).
38. Pourbaix, M., “Atlas d’équilibres électrochimiques,” p. 273. Publication du centre d’étude de la corrosion (CEBELCOR), Gauthier-Villars, Paris, 1963.
39. Vít, Z., and Zdražil, M., *J. Catal.* **171**, 305 (1997).
40. Masson, J., and Neichtschein, J ., *Bull. Soc. Chim. Fr.* **1968**, 3933 (1968).
41. Mulcahy, F. M., Houalla, M., and Hercules, D. M., “Proceedings 9th International Congress on Catalysis, Calgary, 1988” (M. J. Philipps and M. Ternan, Eds.), pp. 1968–1975. Chem Institute of Canada, Ottawa, 1988.
42. Peri, J. B., *J. Phys. Chem.* **69**, 220 (1965).
43. Masson, J., Delmon, B., and Netchschein, J., *C. R. Acad. Sci. C* **266**, 1257 (1968).